AFRL-RV-PS-
TR-2012-0144

A STACKELBERG GAME APPROACH TO COGNITIVE RADIO NETWORK WITH ANTI-JAMMING CAPABILITY

Gerry (Zhi) Tian, et al.

Michigan Technological University
1400 Townsend Dr
Houghton, MI 49931-1200

10 Oct 2012

Final Report

AIR FORCE RESEARCH LABORATORY
Space Vehicles Directorate
3550 Aberdeen Ave SE
AIR FORCE MATERIEL COMMAND
KIRTLAND AIR FORCE BASE, NM 87117-5776

DTIC COPY

NOTICE AND SIGNATURE PAGE

Using Government drawings, specifications, or other data included in this document for any purpose other than Government procurement does not in any way obligate the U.S. Government. The fact that the Government formulated or supplied the drawings, specifications, or other data does not license the holder or any other person or corporation; or convey any rights or permission to manufacture, use, or sell any patented invention that may relate to them.

This report is the result of contracted fundamental research deemed exempt from public affairs security and policy review in accordance with SAF/AQR memorandum dated 10 Dec 08 and AFRL/CA policy clarification memorandum dated 16 Jan 09. This report is available to the general public, including foreign nationals. Copies may be obtained from the Defense Technical Information Center (DTIC) (http://www.dtic.mil).

AFRL-RV-PS-TR-2012-0144 HAS BEEN REVIEWED AND IS APPROVED FOR PUBLICATION IN ACCORDANCE WITH ASSIGNED DISTRIBUTION STATEMENT

//SIGNED//
KHANH PHAM
Program Manager

//SIGNED//
BRETT J. DEBLONK, Ph.D.
Technical Advisor, Spacecraft Component Technology Branch

//SIGNED//
KENNETH D. BOLE, Lt Col, USAF
Deputy Chief, Spacecraft Technology Division
Space Vehicles Directorate

This report is published in the interest of scientific and technical information exchange, and its publication does not constitute the Government's approval or disapproval of its ideas or findings.

Approved for public release; distribution is unlimited.

REPORT DOCUMENTATION PAGE

Form Approved
OMB No. 0704-0188

1. REPORT DATE *(DD-MM-YYYY)*	2. REPORT TYPE	3. DATES COVERED *(From - To)*
10-10-2012	Final report	27 Jul 2011 to 27 Jul 2012

4. TITLE AND SUBTITLE

A Stackelberg Game Approach to Cognitive Radio Network with Anti-Jamming Capability

5a. CONTRACT NUMBER
FA9453-11-1-0290

5b. GRANT NUMBER

5c. PROGRAM ELEMENT NUMBER
61102F

6. AUTHOR(S)

Gerry (Zhi) Tian, Xin Tian*, Dan Shen*, and Genshe Chen*

5d. PROJECT NUMBER
2304

5e. TASK NUMBER
PPM00013856

5f. WORK UNIT NUMBER
EF005737

7. PERFORMING ORGANIZATION NAME(S) AND ADDRESS(ES)

Michigan Technological University
1400 Townsend Dr.
Houghton, MI 49931-1200

*Intelligent Fusion Technology, Inc.
20271 Goldenrod Lane, Suite 2066
Germantown, MD 20876

8. PERFORMING ORGANIZATION REPORT NUMBER
MTU 1104034Z1-Final

9. SPONSORING / MONITORING AGENCY NAME(S) AND ADDRESS(ES)

Air Force Research Laboratory
Space Vehicles Directorate
3550 Aberdeen Ave., SE
Kirtland AFB, NM 87117-5776

10. SPONSOR/MONITOR'S ACRONYM(S)
AFRL/RVSV

11. SPONSOR/MONITOR'S REPORT NUMBER(S)
AFRL-RV-PS-TR-2012-0144

12. DISTRIBUTION / AVAILABILITY STATEMENT

Approved for public release; distribution is unlimited.

13. SUPPLEMENTARY NOTES

14. ABSTRACT

In this work a cognitive jamming/anti-jamming game is investigated in the context of space communication networks. The jamming/anti-jamming problem is formulated as a two sides zero sum game to minimize/maximize the amount of data transmitted over each game period. It takes into account both the detection speed of the jammer's detector and the impact of transmission delays in space communications. The results provide valuable information on the evaluation of jammer's potential impact on communication links in space and support the development of jamming resistant space communication networks.

15. SUBJECT TERMS
Space communication network, cognitive radio, energy detection, game theory

16. SECURITY CLASSIFICATION OF:			17. LIMITATION OF ABSTRACT	18. NUMBER OF PAGES	19a. NAME OF RESPONSIBLE PERSON
a. REPORT	b. ABSTRACT	c. THIS PAGE			Khanh Pham
Unclassified	Unclassified	Unclassified	Unlimited	34	19b. TELEPHONE NUMBER *(include area code)*

Standard Form 298 (Rev. 8-98)
Prescribed by ANSI Std. 239.18

(This page intentionally left blank)

TABLE OF CONTENTS

Section **Page**

LIST OF FIGURES

Figure **Page**

LIST OF TABLES

Acknowledgement

The authors appreciate Dr. Khanh Pham for his support and guidance during this effort.

1 Summary

Spectrum sensing capabilities of cognitive radios can be used by (cognitive) jammers to guide jamming attacks on their targeting communication links. Existing works in the literature assume that cognitive jammers have rather limited hardware resources and processing power, as a result, they can only conduct channel sensing in a sequential manner, i.e., only one communication channel can be sensed at a time. In this work we consider more sophisticated jamming/anti-jamming scenarios that may encountered in military applications, where jammers have powerful spectrum sensing capability and are able to simultaneously monitor communication channels in the operating spectrum. For anti-jamming, the transmitter-receiver side uses the frequency hopping spread spectrum (FHSS) to mitigate the jammer's impact. In this research, using game theoretical approach, novel algorithms are developed to evaluate the impact of cognitive jammers. The results are determined by multiple factors including geometric relationship among the transmitter, receiver and jammer, antenna patterns, detection performance of the jammer's spectrum sensing algorithm, the frequency hopping rate, transmission power, channel bandwidth, etc. The evaluations support the selection of suitable anti-jamming strategies, network topology optimization, transmission power control, channel capacity plan, etc., for the development of jamming resisting communication networks.

2 Introduction

Wireless communication is vulnerable to jamming attacks of which mitigation strategies include Frequency Hopping Spread Spectrum (FHSS) and Direct Sequence Spread Spectrum (DSSS). Cognitive Radios (CRs) with the capability of sensing the spectrum environment were initially developed to allow unlicensed (secondary) users to identify and utilize opportunistic spectrum resources when they are not occupied by licensed users. The same CR technologies developed for spectrum sensing and allocation can be used by jammers for directing attacks to their targeted communication systems. Existing works in the literature assume that cognitive jammers have rather limited hardware resources and processing power, as a result, they can only conduct channel sensing in a sequential manner, i.e., only one communication channel can be sensed at a time [5-8]. In such scenarios, the major decision making of the jammers is focused on determination of which channel or channels (in the case of multiple coordinated jammers) to sense or jam. In this work, we investigate Cognitive Radio (CR) jamming in the context of an anti-jamming game theoretical framework for space communication applications. Here it is assumed that the jammer has enough processing power and resources to simultaneously monitor communication channels in the operating spectrum range. In this research, using game theoretical approach, novel algorithms are developed to evaluate the impact of cognitive jammers. The evaluations support the selection of suitable anti-jamming strategies, network topology optimization, transmission power control, channel capacity plan, etc., for the development of jamming resisting communication networks.

The report is organized as follows. The methods, assumptions, and procedures are presented in section 3. Section 3.1 describes the scenario considered and formulates the basic cognitive jamming/anti-jamming game between the transmitter-receiver and the jammer in space. Section 3.2 presents the design and performance evaluation of the sliding window energy detector. Section 3.3 derives the Maxmin solution of the cognitive jamming/anti-jamming game. Section 4 shows the major results from this research by demonstrating the impacts of propagation delay difference, receiver-jammer side SNR ratio and channel bandwidth on the game solution. Section 5 summarizes the report with concluding remarks.

3 Methods, Assumptions, and Procedures

The focus of this work is to investigate the impact of the jammer's response time (the time for the jammer to detect and react to data transmission from the transmitter to the receiver over a communication channel) on the behaviors of both systems in the jamming/anti-jamming game. To this end the concept of *jammer reaction time* is introduced which accounts for the transmission detection time as well as the difference in signal prorogation time over two different paths (transmitter-receiver and transmitter-jammer-receiver). For channel sensing, it is assumed that the jammer uses a *sliding window energy detector* (SWED) to constantly monitor the communication channels. Energy detection is a commonly used for spectrum sensing approach due to its simplicity and low requirements on information of the transmitter-receiver side [9]. However, energy detection used in a sliding window fashion has not been addressed in the literature, which is an important subject of this work. The jamming/anti-jamming problem is formulated as a zero-sum game between the transmitter-receiver and the jammer. Both sides try to manipulate the jammer's reaction time through their own control variables (transmission power over the communication channel on the transmitter-receiver side and detection sliding window length on the jammer side) to increase/reduce the amount of data transmitted over a game period (time slot). Major contributions of this work are listed as follows: i) A novel approach is developed for performance evaluation of the sliding window energy detector; ii) Performance of the sliding window energy detector is characterized in terms of the distribution of detection time versus detector side signal-to-noise ratio (SNR), which allows the determination of the optimal window length on the jammer side for channel sensing and lays the foundation for the solution of the proposed zero-sum jamming/anti-jamming game; iii) As a conservative strategy of the transmitter-receiver side, Maxmin solutions of the game are obtained for various scenarios to show the impacts of the difference in signal propagation delays, the receiver-jammer side SNR and the channel bandwidth on the game solution. The results reflect the cognitive jammer's capacity in jamming certain communication links in different scenarios and provide important guidance to the development of jamming resisting strategies in space communication networks

3.1 Problem formulation

In this work, the cognitive jamming/anti-jamming problem is formulated in the context of space communications, e.g., the communication between two satellites through an inter-satellite communication link. The basic scenario, as illustrated in Fig. 1, consists of a communication pair of receiver (A) and transmitter (B) and a jammer (C). Communication in space is characterized by large distance between the transmitter and the receiver (typical inter-satellite communication links (ISLs) ranges from several thousand kilometers (ISLs in Low-Earth Orbit (LEO) constellations) to thirty thousand kilometers for Geosynchronous Earth Orbits (GEO) - (LEO-GEO ISLs)) and highly directive antennas with typical antenna beam width of 0.25°. As a result the geometric relationship of the transmitter, receiver, and jammer plays an important role in communication performance. Since the orbit trajectories of the transmitter, receiver, and jammer are highly predictable, for the jamming/anti-jamming problem it is assumed that their relative positions are known (or are within a reasonable spatial accuracy). In Fig. 1,

t_{BA}, t_{BC} and t_{CA} denote the signal propagation time between BA, BC, and CA. In space communications, the signal propagation delays between the transmitter, receiver, and jammer are on the order of tens to hundreds of milliseconds, which are not negligible for the cognitive jamming/anti-jamming problem.

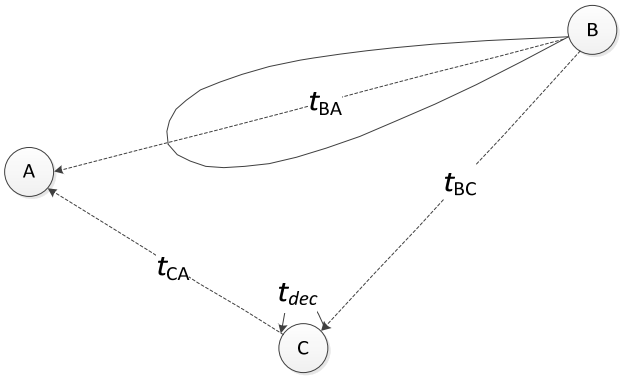

Figure 1. The basic scenario with transceivers A, B, and jammer C

Without loss of generality, it is assumed that there are M independent communication channels available for data transmission from B to A, with each allocated a bandwidth W. The jammer directs its receiving antenna to the transmitter in order to detect data transmission activities from the transmitter to the receiver. It is assumed that the jammer has sufficient processing capability to simultaneously monitor all the M communication channels, and over each channel an energy detector is used in a sliding window fashion for spectrum sensing. Once data transmission is confirmed over a communication channel, the jammer will send a jamming signal to the receiver to block its reception over the communication channel. It is assumed that the jammer is powerful enough to interrupt the receiver's reception over the selected communication channels. The jammer's strategy can be summarized as "detect and jam". In such a strategy, the key factor that determines the jamming results is how fast the jammer is able to react to the data transmission over a communication channel, namely the response time of the jammer, which is defined as

$$t_{res}(i)=t_{BC}+t_{CA}-t_{BA}+t_{dec}(i)=\Delta t_D+t_{dec}(i) \quad (1)$$

It consists of two parts (i) the detection time t_{dec}, which is the time between the transmitting signal from B (over the communication channel) reached the jammer over channel i and the time when the jammer's detector makes the detection, and (ii) the difference of the signal propagation delays over two paths B-A and B-C-A, Δt_D, which is a known constant in a given scenario. The response time in (1) is the period of time that the data transmission can be conducted over channel i unaffected by the jammer. It is of the jammer's interest to minimize the detection time, which, as shown in Sec. 3.2, is jointly determined by the signal-to-noise ratio (SNR) at the jammer side and the window length of the sliding window detector.

To mitigating the jammer's impact, the transmitter-receiver side employs the FHSS strategy with a limited hopping frequency $1/T$, which means that once the transmitter and

receiver starts to use a communication channel, they have to stay with that channel for at least a period time of T before the data transmission can hop to another channel. Note that frequency hopping can occur at 500-1500 Hz, corresponding to a game period of 2ms to 0.7ms, which is much smaller than the signal propagation time from the transmitter to the receiver. As a result the transmitter and receiver will follow a predetermined hopping pattern which can be updated at a low rate by the receiver side based on its local radio-frequency (RF) environment sensing results.

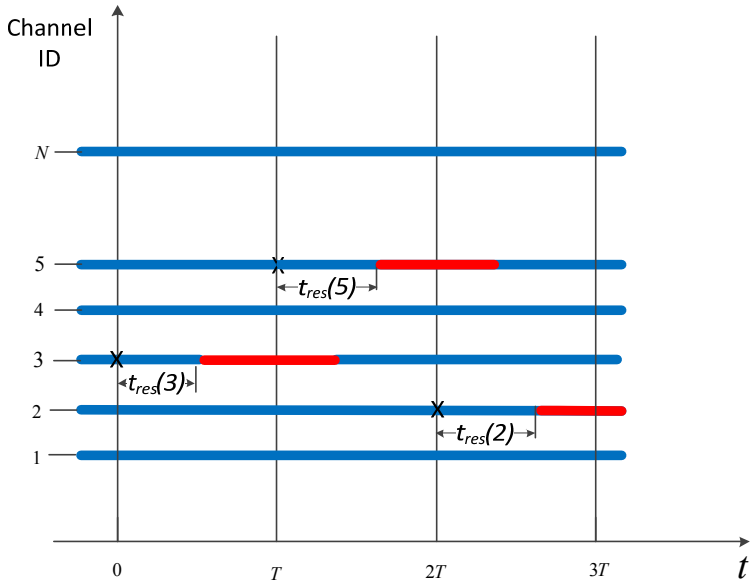

Figure 2. Illustration of the jamming and anti-jamming game

Fig. 2 illustrates the jamming/anti-jamming game process for the case when the transmitter and receiver transmit over only one channel at a time according to the channel hopping pattern indicated by the "X" markers. Note here for the sake of convenience, time at the receiver side is used as the reference time and t_{res} is the response time. The first game period starts from time 0, when the receiver begins to receive data transmission from the transmitter over channel 3 according to the channel hopping pattern. The data transmission goes uninterrupted for a time period of $t_{res}(3)$, then the channel becomes jammed as the jamming signal from C arrives. At time T, the data reception is switched to channel 5 according to the channel hopping pattern, which starts a new round of game.

To maximize the amount of data transmitted during each transmission period (game period) T, the transmitter-receiver side needs to choose an optimal transmission power to maximize the product of the channel capacity and the jammer's response time t_{res}(i) in (1). The jamming/anti-jamming game over channel i is formulated as follows:

$$P_A^{i*} = \arg\max_{T_w^{i*}, P_A^i} \mathrm{E}[C^i t_{res}(i)] = \arg\max_{T_w^{i*}, P_A^i} C^i \mathrm{E}[t_{\mathrm{dec}}(i)] + C^i \Delta t_D \tag{2}$$

$$T_w^{i*} = \arg\min_{T_w^i, P_A^{i*}} \mathrm{E}[C^i t_{res}(i)] = C^{i*} \arg\min_{T_w^i, P_A^{i*}} \mathrm{E}[t_{\mathrm{dec}}(i)] + C^i \Delta t_D \tag{3}$$

$$s.t. \quad t_{res}(i) = t_{\mathrm{dec}}(i) + \Delta t_D \le T, \tag{4}$$

$$P_{FA}(K) = \tau, (e.g., K = 500, \tau = 0.01) \quad (5)$$

$$P_A^i \le P_{\max} \quad (6)$$

where P_B^i, is the transmission power over the channel, which determines the signal power levels at the receiver (P_A^i) and at the jammer (P_C^i); T_w^i is the window length of the jammer's sliding window detector that control the detector's detection performance; and C^i is the theoretical capacity of the communication channel.
From information theory, one has

$$C^i = W^i \log_2(1 + \frac{P_A^i}{N_{A0} W^i}) = W^i \log_2(1 + SNR_A) \quad (7)$$

where $SNR_A = \frac{P_A^i}{N_{A0} W^i}$ is the receiver side signal to noise ratio; W^i is the channel bandwidth, P_A^i is the receiver side signal power, N_{A0} is the receiver side noise power spectrum density and is given by

$$N_{A0} = \kappa T_A \quad (8)$$

where T_A is the receiver system temperature and κ *=1.38e-23* W/Hz-K is the Boltzmann constant.

In space communications, the receiver side signal power P_A^i is related to P_B^i (the transmission power over the channel which is the control variable in (2)) by [1]

$$P_A^i = P_B^i G_{BA} G_{AB} \left(\frac{\lambda}{4\pi R_{AB}} \right)^2 \quad (9)$$

where λ is the wavelength of the signal carrier, G_{BA} and G_{AB} are the transmitter and receiver antenna gains respectively.

In (4), $t_{dec}(i)$ is the jammer's detection time as shown in Sec.3.2 for the sliding window energy detector considered, its distribution is determined by the length of the sliding window T_w^i and the jammer side SNR, which is defined as

$$SNR_C = \frac{P_C^i}{2W^i N_{C0}} \quad (10)$$

where P_C^i is the jammer side signal power which is related to the transmission power by

$$P_C^i = P_B^i G_{BC} G_{CB} \left(\frac{\lambda}{4\pi R_{BC}} \right)^2 \quad (11)$$

and similar to N_{A0} in (8), $N_{C0} = \kappa T_C$ is the noise power density at the jammer's detector. Note that for a given scenario with known geometric relationships among the transmitter, the receiver and the jammer, the ratio of the receiver side and jammer side SNRs is given by

$$\frac{SNR_A}{SNR_C} = \frac{G_{BA} G_{AB} R_{BC}^2 N_{C0}}{G_{BC} G_{CB} R_{BA}^2 N_{A0}} \quad (12)$$

As shown in Sec.4, this receiver-jammer SNR ratio has a big impact on the results of the cognitive jamming/anti-jamming game.

In (2) the transmitter-receiver side tries to select the optimal power over the channel P_A^i to maximize the expected amount of data transmitted over the game period T, which involves two conflicting interests, namely to increase the channel capacity C^i and to increase the expected response time $E[t_{res}(i)]$. In (3), the jammer has the control over the sliding window length of the energy detector T_w^i to minimize the expected detection time $E[t_{dec}(i)]$. The constraint in (4) imposes the constraint of the game period T. The constraint in (5) is the requirement on the cumulative false alarm rate of jammer's the sliding window energy detection over K consecutive tests, which will be discussed in detail in Sec.3.2. Constraint (6) is enforced by the maximum transmission power of the transmitter. Note that the transmitter-receiver side has an incentive of not using a large transmission power to increase the jammer's response time. In most scenarios the transmitter won't choose to use the maximum power and constraint (6) is inactive. Results from the single channel jamming/anti-jamming can be utilized in the case when multiple channels are used simultaneously for data transmission where the decisions of transmitting power levels over different channels are only coupled by a total power constraint. Also note that the "detect and jam" strategy for the jammer is preferred when the total number of communication channels M is significantly larger than the number of channels used for simultaneous data transmission and the number of channels jammer is able to jam at a time. In such scenarios, random jamming strategies [6,7] will have very low jamming probabilities. However there is a point from which the jammer will start favoring a random jamming strategy over the "detect and jam", which will be a subject of future investigation.

3.2 Design and Performance Evaluation of Sliding Window Energy Detection for Spectrum Sensing

In this section we present the design and performance analysis of the sliding window energy detector used by the jammer for the monitoring of the communication channels. Detection performance of the detector is evaluated for various window lengths under different levels of signal noise ratios to support the solution of the jamming/anti-jamming game (2)-(6).

3.2.1 Problem description

Energy detection is one of the most commonly used approaches for spectrum sensing [7]. The detector operates by comparing the energy of the received waveform over a time window to a threshold determined by the noise floor. An energy detector was first investigated in [2] for the detection of unknown deterministic signals over a band limited additive white Gaussian noise (AWGN) channel. Using sampling theory, it was shown that the test statistic of the energy detection follows a chi-square (χ^2) distribution under H_0 (no signal transmission) and the non-central chi-square distribution under H_1 (with signal transmission), based on which the exact false alarm rate and detection probability were derived. In [1, 3], the energy is extended for the detection of unknown signals over different types of fading channels, where closed-form expressions for the detection probabilities over Rayleigh, Nakagami, and Rician fading channels were presented. In [5]

the optimal sensing time of the secondary user using energy detection is derived to maximize the average throughput and protect the primary user from harmful interference. However, the evaluation of the false alarm rates and detection probabilities did not take into account the correlation among the tests over time. As shown in Fig. 3(b) the testing windows in the sliding window test have overlaps, and as a result, test statistics in the sliding window test are correlated over time. In this article, we demonstrate a solution for a sliding window energy detector for correlated tests.

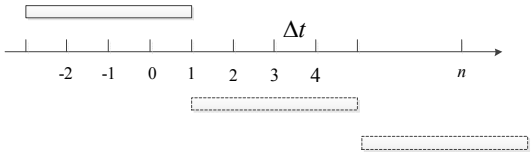

(a) Independent tests

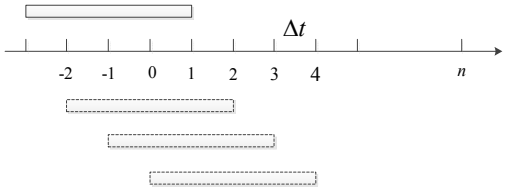

(b) Sliding window tests

Figure 3. Independent tests and sliding window tests

The conventional methods on energy detection as those mentioned above [1-5] assume that the hypothesis tests are independent. However, the assumption only holds when the detection tests use independent data sets from non-overlapping testing windows. As shown in Fig. 3(a), independent tests can only be performed at a rate that is lower than once every time period of the testing window length. When the window length is large (which is particularly necessary when the SNR at the detector's receiver is low), it significantly increases the detection time and degrades detection performance. In addition, with the testing rate related to the window length, it is difficult to conduct a fair performance comparison for tests with different window lengths, since the numbers of tests conducted over a given time period are different. In the SWED test considered in this work, tests are performed at every fixed time interval regardless of the window length. When the testing windows in the sliding window test overlap the test statistics in the sliding window test are correlated over time. This correlation significantly complicates the design and performance analysis of the sliding window test for spectrum sensing. To address the problem, in this paper, first an effective approximation and a numerical method are proposed for the evaluation of the false alarm rate of the SWED. Interestingly, it is observed that the false alarm rate of a sliding window test for energy detection and that of the independent test have a relationship that is almost linear. Based on the results, the design of the sliding window energy test is addressed. Then using the same approaches, detection probabilities of the SWED test are evaluated for given window length and SNR level. The corresponding distribution of the detection time is also obtained, which allows the determination of the optimal window length that minimizes the expected detection time.

The section is organized as follows. Sec. 3.2.2 briefly reviews conventional energy detection under the independent assumption [2]. For the sliding window test using energy detection, Sec. 3.2.3 presents the algorithms for false alarm analysis and proposes the test design process. The evaluation of the detection probability and the analysis of detection performance are presented in Section 3.2.4.

3.2.2 Energy detection under independent assumption

First for readers' convenience, the main notations used in this paper for the description of energy detection are listed as follows, which follow mostly the notations in [1].

$s(t)$: signal waveform.

$n(t)$: noise waveform assumed to be a zero-mean white Gaussian random process.

N_0 : two-sided noise power spectral density

P_s : signal power

W : one-sided bandwidth in Hz, i.e., the positive bandwidth of the low-pass signal.

Δt : sampling and testing interval $= \frac{1}{2W}$.

T : window length of the energy test, which is assumed to consist of a number of segments of Δt.

L : discrete window length = $T / \Delta t$.

η : detector signal noise ratio $= \frac{P_s \Delta t}{N_0} = \frac{P_s}{N_0 2W} = SNR_C$.

τ : threshold used by the energy detector

$N(\mu, \sigma^2)$: Gaussian random process whose probability density function is defined

χ_α^2 : chi-square distribution with α degrees of freedom.

$\chi_\alpha^2(\beta)$: Non-central chi-square distribution with α degrees of freedom and non-centrality parameter β.

For the detection problem, the received waveform is given by

$$y(t) = \begin{cases} s(t) + n(t), & \text{under } \mathrm{H}_1 \\ n(t), & \text{under } \mathrm{H}_0 \end{cases} \tag{13}$$

As shown in [2], for the decision process, the baseband signals and the pass band signals are equivalent for the decision process. For the sake of convenience, as in [1], the received signal is assumed to be at the baseband and has a limited bandwidth W. According to sampling theory [2] one can express the noise process as:

$$n(t) = \sum_{i=-\infty}^{\infty} n[i]\mathrm{sinc}(2Wt - i) \tag{14}$$

where $\text{sinc(x)}=\frac{\sin(\pi x)}{\pi x}$ and $n[i]=n(\frac{i}{2W})=n(i\Delta t)$, which is a discrete white noise random process (sampled from $n(t)$ with sampling interval $\Delta t=\frac{1}{2W}$) with zero mean and variance $2N_0W$, namely,

$$n[i]\sim N(0,2N_0W) \tag{15}$$

Similarly for the signal, one has

$$s(t)=\sum_{i=-\infty}^{\infty}s[i]\text{sinc}(2Wt-i) \tag{16}$$

where $s[i]=s(i\Delta t)$.

For a test using the data in a time window [0 T], the test statistic of the energy detection is given by [2]

$$V=\frac{1}{N_0}\int_0^T y(t)^2dt=\frac{1}{2WN_0}\sum_{i=1}^{2TW}y[i]^2=\frac{1}{2WN_0}\sum_{i=1}^{L}y[i]^2 \tag{17}$$

where $L=2TW=T/\Delta t$ is the window length in discrete time.

It can be easily seen that under H_0

$$\frac{y[i]}{\sqrt{2WN_0}}\sim N(0,1) \tag{18}$$

and as a result

$$V\sim\chi_L^2. \tag{19}$$

Under H_1, one has

$$\frac{y[i]}{\sqrt{2WN_0}}\sim N(\frac{s[i]}{\sqrt{2WN_0}},1) \tag{20}$$

and

$$V\sim\chi_L^2(\lambda), \tag{21}$$

where

$$\lambda=\frac{1}{2WN_0}\sum_{i=1}^{L}s[i]^2=\frac{1}{N_0}\int_0^T s(t)^2dt=\frac{P_sT}{N_0} \tag{22}$$

is the non-centrality parameter.

The probability density function (pdf) of the test statistic is [8, 9]

$$f_V(x)=\begin{cases}\frac{1}{2^{L/2}\Gamma(L/2)}x^{L/2-1}e^{-x/2}, & \text{H}_0\\ \frac{1}{2}e^{-(x+\lambda)/2}(\frac{x}{\lambda})^{L/4-1/2}I_{L/2-1}(\sqrt{\lambda x}), & \text{H}_1\end{cases},\ x\geq 0 \tag{23}$$

where $\Gamma(L/2)$ denotes the Gamma function and $I_v(z)$ is a modified Bessel function of the first kind.

The probability of false alarm P_f (under H_0) and probability of detection P_d (under H_1) are given by [3]

$$P_f = P(V > \tau \mid \mathrm{H}_0) = 1 - \frac{\gamma(L/2, \tau/2)}{\Gamma(L/2)} \tag{24}$$

where $\gamma(k,z)$ is the lower incomplete Gamma function, and

$$P_d = P(V > \tau \mid \mathrm{H}_1) = Q_{\frac{L}{2}}(\sqrt{\lambda}, \sqrt{\tau}) \tag{25}$$

where $Q_M(a,b)$ is the Marcum Q-function [4].

The evaluations of P_f (24) and P_d (25) only apply to energy tests that are independent. For the sliding window test, test statistics of multiple tests are correlated and the above evaluations are no longer valid. In Sec. 3.2.3 and 3.2.4, novel algorithms will be developed to address the problem of correlated test statistics.

3.2.3 False alarm evaluation for sliding window test using energy detection

Suppose the window length of the test is L in discrete time and the tests are conducted at discrete time k, where $k = 1, 2, 3, \ldots$ The corresponding test statistics are

$$V[k] = \frac{1}{2WN_0} \sum_{i=k-L}^{k} y[i]^2 \;<=>\; \frac{1}{N_0} \int_{(k-L)\Delta t}^{k\Delta t} y(t)^2 \, dt \tag{26}$$

Suppose the test starts from k=1, under hypothesis H_0, sliding window false alarm probabilities, P_{fs}, at the following testing times are

$$P_{fs}[1] = P(V[1] > \tau) \tag{27}$$

$$P_{fs}[2] = P(V[2] > \tau \mid V[1] \le \tau) \tag{28}$$

$$P_{fs}[3] = P(V[3] > \tau \mid V[1] \le \tau, V[2] \le \tau) \tag{29}$$

$$P_{fs}[4] = P(V[4] > \tau \mid V[1] \le \tau, V[2] \le \tau, V[3] \le \tau) \tag{30}$$

The evaluation of $P_{fs}[1]$ follows directly (24). However the exact evaluations of the conditional probabilities in (28)-(30) are increasingly more complicated. In this paper the following approximation is used for the evaluation of false alarm rates in sliding window test

$$P_{fs}[k] \approx P(V[k] > \tau \mid V[k-1] \le \tau) = P_{FAs} \tag{31}$$

which is conditioned only on the previous testing result that has the biggest impact on the current test at time k.

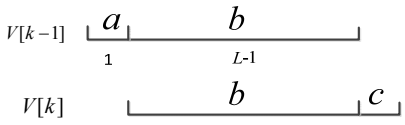

Figure 4. Test statistics of two consecutive tests in the sliding window test

For the evaluation of (31), Fig.4 shows the relationship between two consecutive test statistics where $V_C^i[k-1]=a+b$ is the sum of two independent random variables *a* and *b*. Under H_0 one has $a\sim\chi_1^2$ and $b\sim\chi_{L-1}^2$. $V_C^i[k]=b+c$ is the sum of *b*, which is the common part with $V_C^i[k-1]$ and random variable *c* which follows χ_1^2 and is independent of *b* and *a*.

To evaluate P_{FAs}, the posterior probability density function of *b* conditioned on $V_C^i[k-1]\le\tau$, namely, $p_b(b\,|\,a+b\le\tau)$, needs to be first evaluated. From Bayes' rule, one has

$$p(b\,|\,a+b\le\tau)\propto p_b(b)\int_0^{\tau-b}p_a(a)\mathrm{d}a \tag{32}$$

where $p_a(\cdot)$ denotes the prior pdf of random variable *a* and $p_b(\cdot)$ is the prior pdf of *b*. Then for the evaluation of (31), it follows that

$$P_{FAs}=1-P(V[k]\le\tau\,|\,V[k-1]\le\tau)=1-\int_0^{\tau}\left[p_b(b\,|\,a+b\le\tau)\int_0^{\tau-b}p_c(c)\mathrm{d}c\right]\mathrm{d}b \tag{33}$$

The direct evaluation of (32) is difficult. In this paper a numerical approach is used. Note that the posterior pdf (32) is non-zero only over interval [0 τ] which allows the use of a discrete approximation to accurately represent the pdf. To do this, the interval [0 τ] is evenly divided into *N* pieces whose probability masses are proportional to the probability density (32) at their center (sampling) points. The discrete approximation of $p_b(b\,|\,a+b\le\tau)$ is obtained as

$$p_b[i\,|\,a+b\le\tau]\propto p_b\left(\frac{\tau}{N}(i-\frac{1}{2})\right)\int_0^{\frac{\tau}{N}(N-i-\frac{1}{2})}p_a(a)\mathrm{d}a,\qquad i=1,...,N, \tag{34}$$

and

$$\sum_{i=1}^{N}p_b[i\,|\,a+b\le\tau]=1, \tag{35}$$

To evaluate (33) the following approximation is used

$$\int_0^{\tau}\left[p_b(b\,|\,a+b\le\tau)\int_0^{\tau-b}p_c(c)\mathrm{d}c\right]\mathrm{d}b\approx\sum_{i=1}^{N}p_b[i\,|\,a+b\le\tau]\int_0^{\frac{\tau}{N}(N-i-\frac{1}{2})}p_c(c)\mathrm{d}c \tag{36}$$

From the approximation, the desired level of evaluation accuracy can be achieved by using sufficiently large *N*.

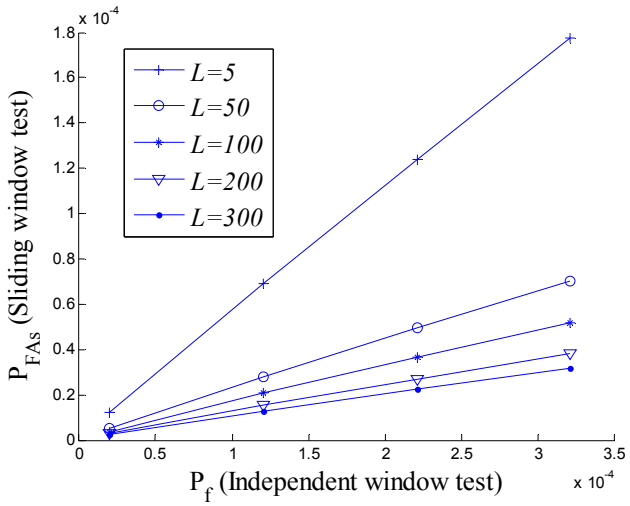

Figure 5. P_{FAs} for the sliding window test vs. P_f for independent window test

Fig. 5 shows P_{FAs} (33) for the sliding window energy test vs. P_f (24) of the independent window test when they use the same window length and the same testing threshold, τ . It can be seen that, for the set of window lengths considered L=5, 50,100, 200, 300, P_{FAs} is smaller than P_f by a reduction factor ranging from 1 (no reduction, when the window length is 1) to approximately 0.1 (for long window lengths up to 300), which is due to the correlation of the tests statistics in the sliding window tests. Interestingly it is observed that for a given window length, P_f vs. P_{FAs} is almost linear, which makes the mapping easy and will greatly simplify the design of sliding window test.

For the design of the sliding window energy test, we are interested in the cumulative false alarm rate over a long period of K consecutive tests, denoted as $P_F(K)$, which is related to P_{FAs} by

$$P_F(K) = 1-(1-P_{FAs})^K \tag{37}$$

For example, when the required cumulative false alarm rate of the jammer's detector is $P_{FA}(500) = 0.01$, the corresponding false alarm rate for sliding window test is giving by

$$P_{FAs} = 1-\left(1-P_F(K)\right)^{1/K} = 2.01\times 10^{-5} \tag{38}$$

Based on the mapping between P_f to P_{FAs} for the window lengths of interest (as shown in Fig. 5), the corresponding P_f can be evaluated, which from (24) leads to the desired test threshold, τ.

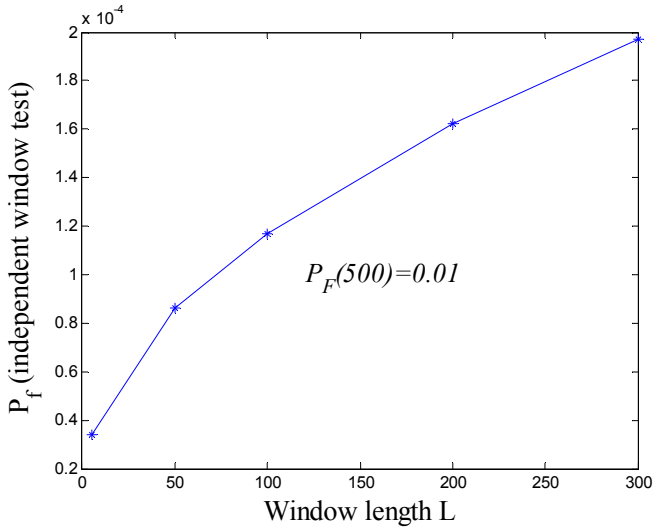

Figure 6. False alarm rates of the corresponding independent window $P_F(500)=0.01$

Fig. 6 shows when $P_F(500)=0.01$, the false alarm rates of the independent tests P_f vs. the window length L. It can be seen that under the same cumulative false alarm rate requirement for the sliding window tests, a larger window length L allows a higher false alarm rate P_f of the corresponding single independent test.

3.2.4 The evaluation of detection probability of sliding window test using energy detection and performance analysis

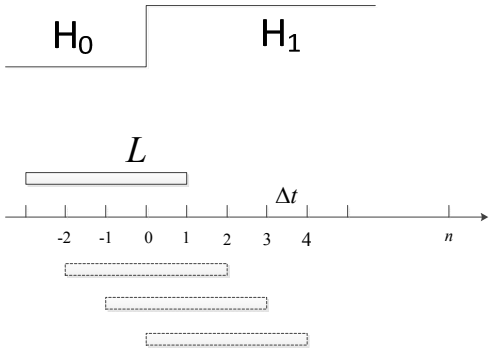

Figure 7. An illustration of the detection process of the sliding window test

Most works on energy tests in the literature assume that under H_1, the signal exists all the time during the tests. In this paper, we investigate the case of detecting the transition from H_0 to H_1 and show the impact of window length on the detection performance. Fig. 7 illustrates the detection process when the sliding window length L=4, and without loss of generality the transition from H_0 to H_1 occurs at 0. The detection probabilities of the sliding window test, P_{ds}, are

$$P_{ds}[1] = P(V[1] > \tau \mid V[0] \le \tau, V[-1] \le \tau, V[-2] \le \tau) \tag{39}$$

$$P_{ds}[2] = P(V[2] > \tau \mid V[1] \le \tau, V[0] \le \tau, V[-1] \le \tau) \tag{40}$$

$$P_{ds}[3] = P(V[3] > \tau \mid V[2] \le \tau, V[1] \le \tau, V[0] \le \tau) \tag{41}$$

where the test statistics $V[k]$ are from (26) and the testing threshold τ is determined based on the requirement on the cumulative false alarm rate for the sliding window test (37) using the design procedure proposed in Sec. 3.2.3. As the case of the false alarm evaluation, the exact evaluations of these detection probabilities are very complicated especially for long window lengths. Instead the same approximation proposed in Sec. 3.2.4 is used for the evaluation of sliding window detection probabilities, i.e.,

$$P_{ds}[k] \approx P(V[k] > \tau \mid V[k-1] \le \tau) = P_{Decs} \tag{42}$$

The same approach for the evaluation of false alarm of the sliding window test can be used for the evaluation of the detection probabilities. The two consecutive test statistics under H_1 bear the same relationship as illustrated in Fig. 4. Similar to (33) one has

$$P_{Decs} = 1 - P(V[k] \le \tau \mid V[k-1] \le \tau) = 1 - \int_0^{\tau} \left[p_b(b \mid a + b \le \tau) \int_0^{\tau - b} p_c(c) \mathrm{d}c \right] \mathrm{d}b \tag{43}$$

But under H_1 the posterior density $p_b(b \mid a + b \le \tau)$ is evaluated under the condition that

$$a \sim \chi_1^2(h\eta), \qquad h = 0,1 \tag{44}$$

where h is 0 when at k-1 there is no signal exists in the first Δt portion of the testing window, otherwise h=1, and

$$\eta = \frac{P_s \Delta t}{N_0} = \frac{P_s}{N_0 2W} = SNR_C \tag{45}$$

is defined as the jammer (detector) side signal noise ratio.

For the common part b of $V[k\text{-}1]$ and $V[k]$ (see Fig. 4) one has

$$b \sim \chi_{L-1}^2(m\eta), \quad m = 1, \ldots, L-1 \tag{46}$$

where m is determined by the number of Δt when the signal exists in the b portion of the testing window.

And under H_1, c follows $\chi_1^2(\eta)$. To evaluate (43), the same numerical approach as in (36) is used.

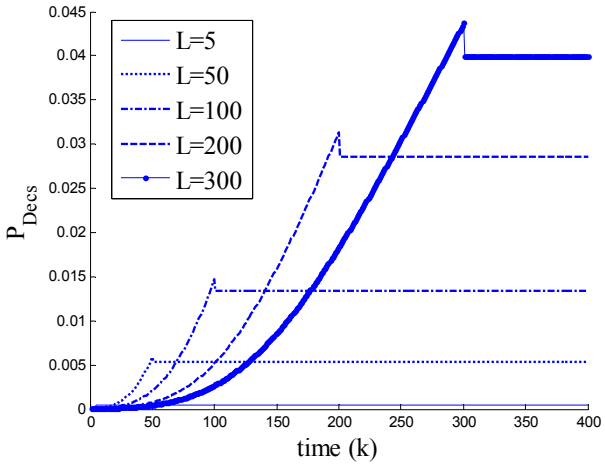

Figure 8. Detection probabilities of sliding window test P_{Decs} vs. time when $\eta = 0.4$ and $P_F(500)=0.01$

Assuming the switch from H_0 to H_1occured at time 0, Fig. 8 shows the detection probabilities of sliding window test for a set of window lengths (L=5,50,100,200,300) from discrete testing times 1 to 400 when the unit time signal noise ratio (45) is 0.4 and the required cumulative false alarm rate $P_F(500)=0.01$. It can be seen that, for a given window length, after the switching from H_0 to H_1, the detection probabilities increase as the signal containing portion of the testing window increases. *The detection probability reaches its peak when the signal portion fills the whole window length*. As the window length increases, the peak detection probability of the sliding window test increases, however, the rate of the increase in detection probability decreases. After reaching the peak detection probability, the detection probabilities of the following tests drop a certain amount due to correlations between the consecutive tests. It can be seen that different window lengths have different tradeoffs between the speed of the detection and the achievable detection probability.

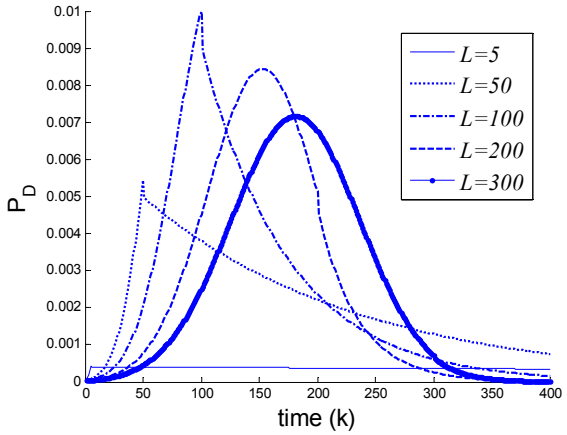

Figure 9. Probability mass function of detection time for the set of window lengths when $\eta = 0.4$ and $P_F(500)=0.01$

Fig. 9 shows the distributions of detection time for the set of window lengths considered over a time period of 400 testing times. The probability mass function of detection time is obtained from P_{Decs} (43) by

$$P_D(k) = \prod_{i=1}^{k-1}(1 - P_{Decs}(i))P_{Decs}(k) \tag{47}$$

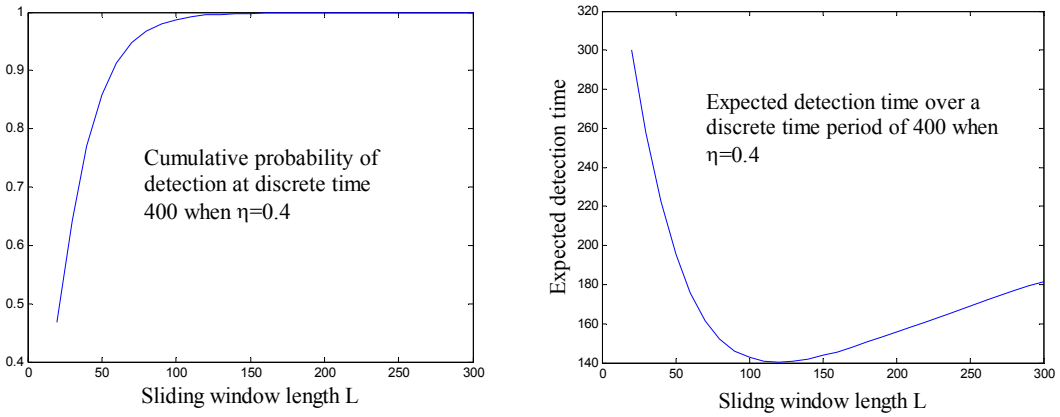

(a) Cumulative probability of detection at time 400. **(b) Expected detection time.**

Figure 10. Detection performance vs. sliding window length when $\eta = 0.4$ and $P_F(500)=0.01$

For window lengths ranging from 20 to 300, Fig. 10(a) shows the cumulative probabilities of detection at the end of the testing period 400; Fig.10 (b) shows their expected detection time. Note that when there is no detection during the testing which occurs quite often with small window lengths (as indicated in Fig.10 (a)), the detection time is counted as 400. It can be seen, for the given unit time signal to noise ratio the expected time vs. the sliding window length takes a convex curve. When $\eta = 0.4$ and $P_F(500)=0.01$, the optimal window length for the sliding window energy detection which minimizes the expected detection time is L=120.

3.2.5 Sliding window energy detection for spectrum sensing summary

This section investigated performance of the energy detection when used in the sliding window test. Unlike conventional independent energy tests, test statistics in the sliding window test are correlated over time, which complicates the design of the test and the evaluation of the testing performance. In this work, algorithms are proposed to effectively evaluate the false alarm rate and the detection probability of the sliding window energy detection. It is observed that, with the same window length, the false alarm rate of the sliding window energy test and that of the independent test have a relationship that is almost linear. Then the distribution of the detection time is obtained for given window length (L) and SNR, which allows the evaluation of the impact of window length on the performance of the sliding window test. It is shown that for the detection of the switching from H_0 to H_1, the choice of window length involves the tradeoff between detection speed and the achievable detection probability. The optimal window length that minimizes the expected detection time under given SNR and false alarm requirement is also obtained. The results will be used to determine the choice the sliding windows in the jamming-antijamming game formulated in Sec. 3.1.

3.3 Maxmin solution to the jamming and antijamming game

As the conservative strategy for the transmitter-receiver side, here we obtain the solution for the following Maxmin game in (48)-(50) to demonstrate the impact of Δt_D, the receiver-jammer side SNR ratio (12) and the channel bandwidth on the results of the cognitive jammig-antijamming game. The Maxmin game is formulated as follows:

$$\begin{aligned} P_A^{i*} &= \arg\max_{P_A^i}\left(\min_{T_w^i} \mathrm{E}[C^i t_{res}(i)](P_A^i, T_w^i)\right) \\ &= \arg\max_{P_A^i}\left(C^i \min_{T_w^i} \mathrm{E}[t_{dec}(i)](P_A^i, T_w^i) + C^i \Delta t_D\right) \end{aligned} \tag{48}$$

$$s.t. \quad t_{res}(i) \le 400\Delta t, \tag{49}$$

$$P_F(500) = 0.01 \tag{50}$$

where $\mathrm{E}[t_{dec}(i)](P_A^i, T_w^i)$ shows explicitly that the expected detection time at the jammer is determined by the reciever side signal power and the window length used by the jammer's detector.

From the discussion in Sec.3.2, the expect detection time is determined by the jammer side SNR (SNR_C) in (45) and from (7) one has

$$\frac{C^i}{W^i} = \log_2(1 + SNR_A) \tag{51}$$

namely the channel's bandwidth efficiency is determined directly by the receiver side SNR. The two SNR values are related by a SNR ratio in (12), which is fixed for a given scenario. Based on the facts above, the game in (48)-(50) is equivalently reformlated as follows to emphasize the essense of the problem

$$SNR_A^{i*} = \arg\max_{SNR_A^i}\left(\left\lfloor \min_{T_w^i} \frac{C^i}{W^i} \mathrm{E}[t_{dec}(i)](SNR_A^i, T_w^i) + \frac{C^i}{W^i}\Delta t_D \right\rfloor / T\right) \tag{52}$$

$$s.t. \quad t_{res}(i) \le 400\Delta t, \tag{53}$$

$$P_F(500) = 0.01 \tag{54}$$

i.e., the transmitter-receiver side chooses the best level of the receiver side signal noise ratio SNR_A to maximize the effective bandwith efficiency (in bit/s/Hz) over the communication channel.

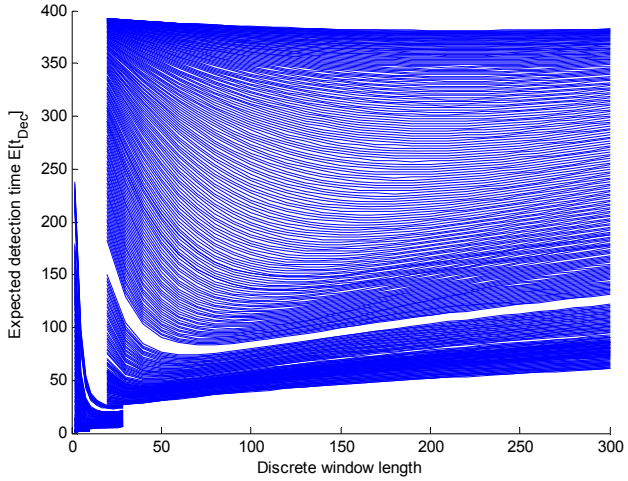

Figure 11. Sliding window length vs. the expected detection time (in discrete time) for jammer side SNR ranging from 0.15 to 15 ($P_F(500)=0.01$).

To evaluate $E[t_{dec}(i)]$, Fig. 11 shows the detection window length T_W vs. the expected detection time $E[t_{dec}]$, which is obtained based on the results in Sec. 3.2 for a wide range of jammer side SNR from 0.15 to 15 under the false alarm requirement $P_F(500)=0.01$. In Fig. 11, the larger jammer side SNR values correspond to lower curves with smaller expected detection time. Note that for the game period of 400 time steps, the range of SNR value is sufficient. When SNR_C is about 0.15 the expected detection time approaches the game period 400 and from the transmitter's perspective once the jammer side SNR reaches 0.15, it won't benefit through further reducing the receiver side SNR. When the SNR_C reaches 15, the expected detection time is close to 1, and the increase of SNR_C won't further reduce the detection time.

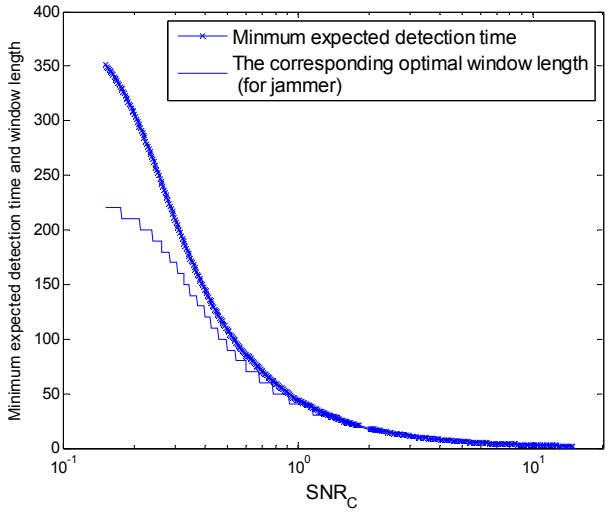

Figure 12. the minimum expected detection time vs. jammer side SNR (PF(500)=0.01, T=400Δt).

Fig. 12 shows the minimum expected detection time of the sliding window detector and the corresponding optimal sliding window length for the range of the jammer side SNR values, which were obtained from the results in Fig. 11. Using (51) and the data shown in Fig. 12, we are ready to evaluate the utility function in (52) and solve the Maxmin game.

4 Results and Discussion

Based on the development in Sec. 3, i.e., the cognitive jamming/anti-jamming problem formulation, jammer side detection performance analysis, and game solution to the cognitive jamming/anti-jamming problem, we are able to evaluate the impacts of three factors (i.e., the time delay difference of the two paths: transmitter-receiver and transmitter-jammer-receiver, the receiver-jammer side SNR ratio, and the channel bandwidth) that determine the game solutions and the achievable channel efficiency of the transmitter-receiver side (52).

4.1 The impact of the difference in signal propagation delay on the Maxmin game solution

Suppose the channel bandwidth is W^i=100kHz. One has the discrete sampling time $\Delta t=5*10^{-6}$s and the corresponding game period is $T=400*\Delta t=2$ms. Here we first fix the SNR ratio (12) at 20 dB. Fig. 13 shows the utility function (52), i.e., the expected bandwidth efficiency (in bit/s/Hz) vs. the receiver side SNR for different Δt_D (1).

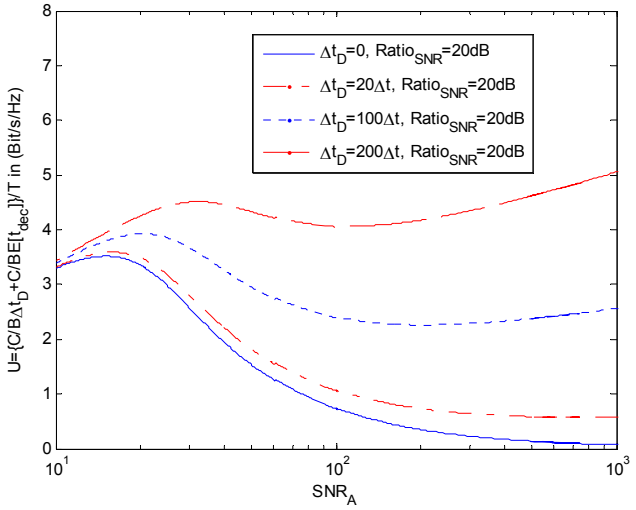

Figure 13. The expected bandwidth efficiency vs. receiver side SNR (SNR ratio=20dB)

As shown in Fig. 13 as the receiver side SNR increases, the expected bandwidth efficiency of the channel first increases, then decreases. For $\Delta t_D>0$, the expected bandwidth efficiency will start to increase again when the receiver side SNR is above a certain level. And for larger Δt_D the optimal SNR level also increases. Table 1 shows the detailed results at the Maxmin solutions for the set of Δt_D considered including the optimal receiver side SNR (SNR_A), the correspoding jammer side SNR (SNR_C), the expected jammer's detection time $E[t_{dec}]$, the receiver side signal power to noise density ratio (P_A/N_0), the expected (theoretical) bandwith efficiency as the utility function in (52), and the expected (theoretical) amount of information transmitted over the channel per game period.

Table 1. Maxmin game solutions when the receiver-jammer side SNR ratio is 20dB

Δt_D	SNR_A (opt)	SNR_C (opt)	$E[t_{dec}]$	P_A/N_0	Utility	Info/T
$\Delta t_D = 0\ \Delta t$	11.8 (dB)	-8.2(dB)	$351\Delta t$	61.8(dBWHz)	3.59 (bit/s/Hz)	700 bit/T
$\Delta t_D = 20\ \Delta t$	12.0 (dB)	-8 (dB)	$332\Delta t$	62 (dBWHz)	3.8 (bit/s/Hz)	760 bit/T
$\Delta t_D = 100\ \Delta t$	13.1 (dB)	-6.9 (dB)	$255\Delta t$	62.18 (dBWHz)	3.95 (bit/s/Hz)	790 bit/T
$\Delta t_D = 200\ \Delta t$	35.2 (dB)	15.2(dB)	$1.1\Delta t$	81.726 (dBWHz)	5.9 (bit/s/Hz)	1180bit/T

As Δt_D increases, the expected detection time will have less impact on the amount of data transmitted over the game period and the optimal SNR value increases for more channel capacity. As shown in bottom row of the table, for the range of receiver side SNR cosidered in the scenario (up to 35.2dB), when $\Delta t_D = 200\Delta t$, the tramsmitter-reciever side will use the largest SNR level and with expected detection time close to 1, the majority of the data will be transmitted during the Δt_D period. Note that when $\Delta t_D \geq T$, one has the jammer's response time t_{res} in (1) always greater than the game period T. As a result the jammer will not be able to follow the channel hopping rate no matter how fast its detection speed is. In such cases, the "detect and jam" strategy is ineffective and the jammer will have to use a random jamming strategy.

4.2 The impact of the receiver-jammer side SNR ratio on the Maxmin game solution

As defined in (12) the receiver-jammer side SNR ratio is determined by the receiver-transmitter, jammer-transmitter, transmitter-receiver and transmitter-jammer antenna gains, the receiver-transmitter and jammer-transmitter distances, and the jammer and receiver side noise spectrum denisties. Assuming $\Delta t_D = 20\Delta t$, Fig. 14 shows the uitility function vs. receiver side SNR for 3 levels of SNR ratios.

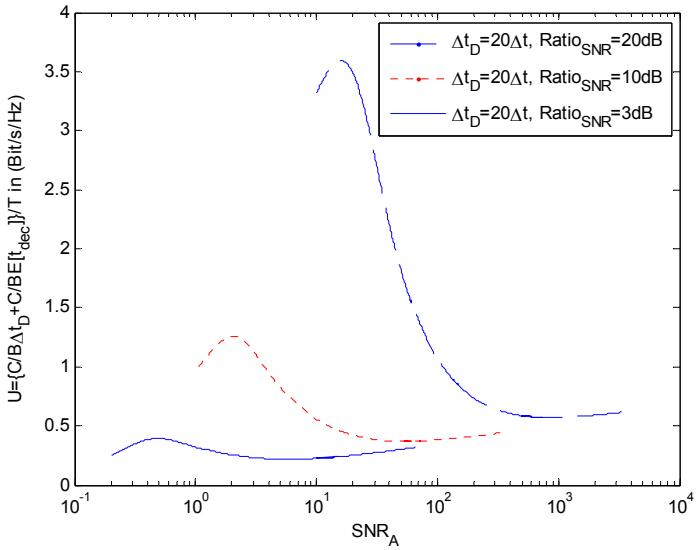

Figure 14. The expected bandwidth efficiency per game period vs. receiver side SNR ($\Delta t_D = 20\Delta t$)

It can be seen that the *SNR* ratio has a significant impact on the game results. Table 2 shows the detailed results at the optimal transmitter side SNR levels from the Maxmin game.

Table 2. Maxmin game solutions when the receiver-jammer side for different SNR ratios ($\Delta t_D=20\Delta t$)

SNR_A/SNR_C	SNR_A (opt)	SNR_C (opt)	$E[t_{dec}]$	P_A/N_0	Utility (opt)	Info/T
20 dB	12 (dB)	-8 (dB)	332Δt	62(dBWHz)	3.8(bit/s/Hz)	760 bit/T
10 dB	3.09 (dB)	-6.91 (dB)	294Δt	53 .09 (dBWHz)	1.26 (bit/s/Hz)	252 bit/T
3 dB	-3.17 (dB)	-6.17 (dB)	258.0Δt	46.83 (dBWHz)	0.39 (bit/s/Hz)	78 bit/T

The results show that when the SNR ratio decreases, the optimal SNR level at the jammer side increases in order to reduce the loss in channel capacity and the expected detection time decreases. The expected bandwidth efficiency and the expected amount of information transmitted per game period significantly deceases with the SNR ratio.

4.3 The impact of channel bandwidth on the game solutions

In the scenarios considered above we assumed that the channel's bandwidth is W=100kHz. From (52) the bandwidth efficiency of a channel is determined by the receiver side SNR_A. For a given bandwidth efficiency, the receiver and jammer side SNRs, i.e., SNR_A and SNR_C are determined. As long as the bandwidth efficiency is fixed, changes in channel bandwidth have no impact on the game solution in discrete time. However the increase in bandwidth decreases the sampling interval. For example, in the previous setup the channel bandwidth was 100k Hz. The sampling interval is $5*10^{-6}$s. The game period of 400 time steps in discrete time corresponds to an actual game period of T=400*Δt=2ms. When the channel bandwidth increases to 1MHz, the sampling interval becomes $5*10^{-7}$s and the game period reduces to 0.2 ms. It can be concluded that channel bandwidth changes the time scale of the game period; the higher the channel bandwidth, the smaller the time scale of the game solution.

5 Conclusions

In this work a cognitive jamming/anti-jamming game is investigated in the context of space communication networks. It is assumed that a cognitive jammer is able to simultaneously monitor the communication channels and uses a "detect and jam" strategy to interrupt the communication between the transmitter and the receiver. For anti-jamming transmitter-receiver side uses frequency hopping with a limited hopping rate. The jamming/anti-jamming problem is formulated as a two sides zero sum game to minimize/maximize the amount of data transmitted over each game period. It takes into account both the detection speed of the jammer's detector and the impact of transmission delays in space communications. To detect data transmission over a communication channel, it is assumed that a sliding energy detector (SWED) is used by the jammer. The transmitter-receiver side has the control over the transmission power, while the jammer with a requirement on false alarm rate has the control over the sliding window length for the detection. To address the design and performance evaluation of the SWED novel algorithms are developed, which accounts for the cross-correlation of the sliding window tests conducted over time. The detection performance is evaluated in terms of the expected detection time under different jammer side SNR and the sliding window length of the detector. As the conservative strategy for the transmitter-receiver side, the Maxmin game solutions are obtained for various scenarios. The impacts of three factors (i.e., the time delay difference of the two paths: transmitter-receiver and transmitter-jammer-receiver, the receiver-jammer side SNR ratio, and the channel bandwidth,) that determine the game solutions and the achievable channel efficiency of the transmitter-receiver side are analyzed. The results provide valuable information on the evaluation of jammer's potential impact on communication links in space and support the development of jamming resistant space communication networks.

References

[1] J. P. Silver, "Satellite Communications Tutorial," john@rfic.co.uk, http://www.odyseus.nildram.co.uk/Systems_And_Devices_Files/Sat_Comms.pdf, accessed 20 August 2012.

[2] M. O. Kolawole, *Satellite Communication Engineering*, Marcel Dekker, Inc. 2002.

[3] F. F. Digham, M.-S. Alouini and M. K. Simon, "On the energy detection of unknown signals over fading channels," *in Proc. of IEEE Internation Conference on Communications (ICC'03)*, pp. 3575–3579, May 2003.

[4] H. Urkowitz, "Energy detection of unknown deterministic signals," *Proc. IEEE,* Vol. 55, pp. 523–531, April 1967.

[5] Q. Wang, P. Xu, K. Ren, and X.-Y. Li, "Delay-bounded adaptive ufhbased anti-jamming wireless communication," in *Proc. IEEE INFOCOM' 11*, 2011, pp. 1413–1421.

[6] Y. Wu, B. Wang, K. J. R. Liu, and T. C. Clancy, "Anti-Jamming Games in Multi-Channel Cognitive Radio Networks," *IEEE Journal on Selected Areas in Communications*, Vol. 30, No. 1, pp.1--12, Jan. 2012.

[7] W. Arbaugh, "Improving the latency of the probe phase during 802.11 handoff," online at www.umiacs.umd.edu/partnerships/ltsdocs/Arbaug talk2.pdf.

[8] T. Shu and M. Krunz, "Throughput-efficient sequential channel sensing and probing in cognitive radio networks under sensing errors," in *Proc. MobiCom'09*, 2009, pp. 37–48.

[9] I. F. Akyildiz et al, "NeXt generation/dynamic spectrum access/cognitive radio wireless networks: a survey," *Computer Networks*, vol. 50, no. 13, pp. 2127 – 2159, Sep. 2006.

LIST OF ACRONYMS, ABBREVIATIONS, AND SYMBOLS

ACRONYM	Description
AWGN	Additive White Gaussian Noise
CR	Cognitive Radio
DSSS	Direct Sequence Spread Spectrum
FHSS	Frequency Hopping Spread Spectrum
GEO	Geosynchronous Earth Orbit
ISL	Inter Satellite Link
LEO	Low-Earth Orbit
SNR	Signal Noise Ratio
SWED	Sliding Window Energy Detector
RF	Radio Frequency

DISTRIBUTION LIST

DTIC/OCP
8725 John J. Kingman Rd, Suite 0944
Ft Belvoir, VA 22060-6218 1 cy

AFRL/RVIL
Kirtland AFB, NM 87117-5776 2 cys

Official Record Copy
AFRL/RVSV/Khanh Pham 1 cy